J. Biochem. **129**, 943–948 (2001)

Demonstration of the Importance and Usefulness of Manipulating Non-Active-Site Residues in Protein Design[1]

Akie Shimotohno,*,† Shinya Oue,† Takato Yano,† Seiki Kuramitsu,* and Hiroyuki Kagamiyama†,[2]

**Department of Biology, Graduate School of Science, Osaka University, Toyonaka, Osaka 560-0043; and †Department of Biochemistry, Osaka Medical College, Takatsuki, Osaka 569-8686*

Received January 12, 2001; accepted March 27, 2001

Do non-active-site residues participate in protein function in a more direct way than just by holding the static framework of the protein molecule? If so, how important are they? As a model to answer these questions, ATB17, which is a mutant of aspartate aminotransferase created by directed evolution, is an ideal system because it shows a 10^6-fold increase in the catalytic efficiency for valine but most of its 17 mutated residues are non-active-site residues. To analyze the roles of the mutations in the altered function, we divided the mutations into four groups, namely, three clusters and the remainder, based on their locations in the three-dimensional structure. Mutants with various combinations of the clusters were constructed and analyzed, and the data were interpreted in the context of the structure-function relationship of this enzyme. Each cluster shows characteristic effects: for example, one cluster appears to enhance the catalytic efficiency by fixing the conformation of the enzyme to that of the substrate-bound form. The effects of the clusters are largely additive and independent of each other. The present results illustrate how a protein function is dramatically modified by the accumulation of many seemingly inert mutations of non-active-site residues.

Key words: directed evolution, protein design, protein engineering, domain motion.

We created a mutant of *Escherichia coli* aspartate aminotransferase (AspAT), named ATB17, by directed evolution, which shows a 10^6-fold increase in the catalytic efficiency for β-branched amino acids, and subsequently determined the crystal structure of ATB17 complexed with a valine analog (*1, 2*). The directed evolution was based on a selection system using an *E. coli* strain that is deficient in the branched-chain amino acid aminotransferase and proved to be a very powerful method of protein engineering. The most unexpected and important finding in this series of studies is that most of the mutated residues are located outside the active site. Although the crystal structure showed that the mutant underwent significant changes in the tertiary and quaternary structures, the questions of which mutations cause the structural changes and how the structural changes in turn affect the activity remain largely unanswered. Elucidation of the causality among these events should deepen our understanding of the structure–function relationship of proteins and benefit future rational, or structure-based, design of protein function.

To fully analyze the effects of the 17 mutated residues of ATB17, we need to make and characterize more than 10^5 (2^{17}) mutants, which is practically impossible. We noticed, however, that many mutated residues are clustered in distinct regions of the three-dimensional structure. In the present study, the mutated residues are grouped as follows (see also Fig. 1): cluster A (Phe24Leu, Asn34Asp, Ile37Met, and Lys41Asn) is located at the "lid" of the active site; cluster B (Ser139Gly and Asn142Thr) is at the "bottom" of the active site; and cluster C (Ile353Thr, Ser361Phe, Ser363Gly, Val387Leu, and Met397Leu) is at the domain interface. Three mutated residues (Ala11Thr, Ala293Val, and Asn297Ser) that do not form a cluster but are known to enhance the activity for β-branched substrates (*2*) are named M. First, the mutations of M are introduced into the wild-type AspAT (WT), then all the combinations of the three clusters are added to M. Analysis of the resultant mutants should reveal how, and to what extent, each cluster contributes to the structural and functional changes observed in ATB17. Three remaining mutations of ATB17 (Lys126Arg, Ala269Thr, and Ser311Gly) were omitted in this study because these were assumed to be functionally neutral mutations because of their locations on the protein surface and their negligible effect on the activity (*1*). To our knowledge, no other mutant enzymes created by directed evolution have been analyzed in such detail.

[1] This work was supported in part by the Ministry of Education, Science, Sports, and Culture of Japan [a Grant-in-Aid for Scientific Research (to T.Y.)], and the Japan Society for the Promotion of Science ["Research for the Future" Program (to H.K.)].

[2] To whom correspondence should be addressed. Fax: +81-726-84-6516, E-mail: med001@art.osaka-med.ac.jp

Abbreviations: AspAT, aspartate aminotransferase; M, AspAT that contains Ala11Thr, Ala293Val, and Asn297Ser mutations; MA, AspAT that contains Phe24Leu, Asn34Asp, Ile37Met, and Lys41Asn mutations in addition to those of M; MB, AspAT that contains Ser139Gly and Asn142Thr mutations in addition to those of M; MC, AspAT that contains Ile353Thr, Ser361Phe, Ser363Gly, Val387Leu, and Met397Leu mutations in addition to those of M; MAB, AspAT that contains the mutations of M, A, and B; MAC, AspAT that contains the mutations of M, A, and C; MBC, AspAT that contains the mutations of M, B, and C; MABC, AspAT that contains the mutations of M, A, B, and C; WT, wild-type AspAT.

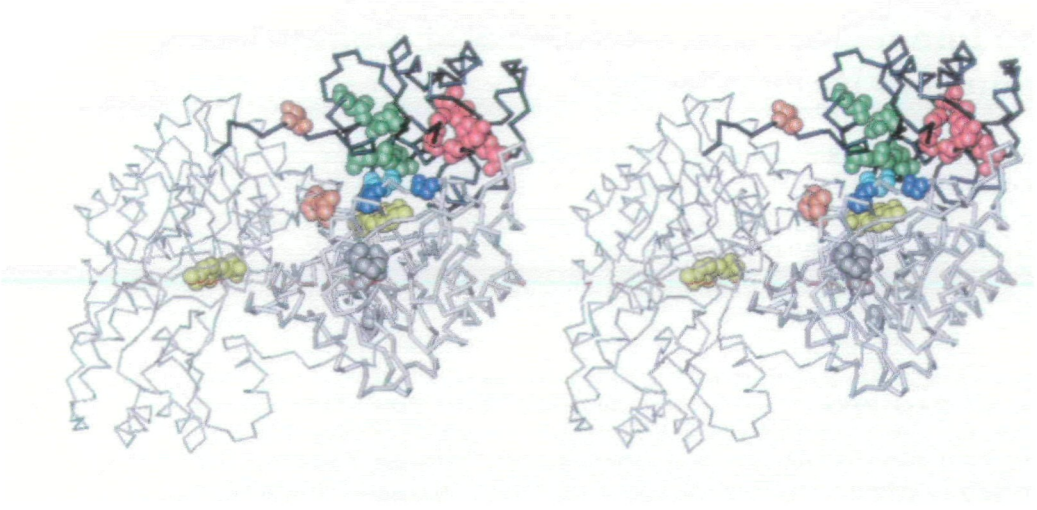

Fig. 1. **Structure of the ATB17–isovalerate complex and the location of the mutated residues (2).** One subunit of the dimer is indicated by a thick line (the small domain is in black), and the mutated residues and the bound valine analog, isovalerate (light blue), are shown only for this subunit. The coenzyme, pyridoxal 5′-phosphate (yellow), is shown for both of the subunits. Grouping of the mutated residues is as follows: Cluster A (green), cluster B (dark blue), cluster C (red), and M (orange). Three mutations of ATB17 that are not included in MABC are in gray.

MATERIALS AND METHODS

Construction of the M, MA, MB, and MC aspC Genes—The wild-type *aspC* gene (*3*) including its cognate promoter was subcloned into a phagemid, pUC118, and its single-stranded (ss) DNA was prepared. Site-directed mutagenesis was performed on the ssDNA using the "Sculptor *in vitro* mutagenesis system" (Amersham Pharmacia Biotech). Two primers were added in a single reaction to introduce three mutations of M simultaneously: 5′-GCAGGAGCGGTGGTAATGTTC-3′ and 5′-TGCTGGTGGGCTAGAGTAGTTAACGCGAATCGCCGC-3′ (mismatches are underlined). The ssDNA of pUC118-M was prepared and used for further mutagenesis. The primers used were: 5′-TCGGCACGAAGCAGATCGGCC-3′ and 5′-CGTCTCATCGTTATAGACACCCATCCCGAGGTCAATTTTGCC-3′ for MA; 5′-GCTCTTATGGGTCGGCCAGCCTGGGTTGCTC-3′ for MB; and 5′-CTGTTTGATGGTAAAGCTGAAG-3′, 5′-GTCAGGCCACCGAAGAAGAACATGCC-3′, 5′-CCACATTTAGGCGACCAGAAGC-3′, and 5′-CAGCGGAGCCAAGTTATCTGGTG-3′ for MC (mismatches are underlined). Nucleotide sequences of the entire coding regions of all the mutant genes reported in this study were verified using a "Dye Terminator Cycle Sequencing Kit" (PE Biosystems) and an ABI "PRIZM" 377A DNA sequencer.

Construction of the MAB, MAC, MBC, and MABC aspC Genes—The *Mlu*I–*Nco*I fragment of MB was ligated into the corresponding restriction sites of pUC118-MA or pUC118-MC to construct pUC118-MAB or pUC118-MBC, respectively. Similarly, the *Mlu*I–*Sal*I fragment of MC was ligated into pUC118-MA to construct pUC118-MAC; and the *Nco*I–*Sal*I fragment of MC was ligated into pUC118-MAB to construct pUC118-MABC.

Expression, Purification, and Enzymological Characterization of AspATs—Each mutant AspAT was expressed in an *aspC*-deficient *E. coli* strain, TY103 (*4*), and purified as described (*5*). The overall transamination reaction between two different amino acids, A and B, is:

$$\text{aa-A} + \text{oxo-B} \rightleftarrows \text{oxo-A} + \text{aa-B}$$

where aa-X and oxo-X are an amino acid, X, and its corresponding 2-oxo acid, respectively. This overall reaction consists of two half-transamination reactions (*6*):

$$\text{EL} + \text{aa-A} \rightleftarrows \text{EL·aa-A} \rightleftarrows \text{EM·oxo-A} \rightleftarrows \text{EM} + \text{oxo-A}$$

$$\text{EM} + \text{oxo-B} \rightleftarrows \text{EM·oxo-B} \rightleftarrows \text{EL·aa-B} \rightleftarrows \text{EL} + \text{aa-B}$$

where EL and EM are the pyridoxal 5′-phosphate form and the pyridoxamine 5′-phosphate form of AspAT, respectively. The activity for each substrate was measured by spectroscopically monitoring the single-turnover of a half-transamination reaction using an Applied Photophysics stopped-flow apparatus, model SX.17MV, as described (*6*). The activity for the overall transamination reaction was measured by coupling malate dehydrogenase as described (*7*), except that 2-oxoleucine was used in place of 2-oxoglutarate. The dissociation constants of AspATs for maleate were measured by spectrophotometric titration (*8, 9*): the absorption spectrum of AspAT, which derives from the coenzyme molecule, is known to change upon binding of maleate to the enzyme. All the enzymological measurements in this study were done at 25°C in the buffer system of 50 mM Hepes, pH 8.0, containing 0.1 M KCl and 10 μM EDTA.

RESULTS

Enzymatic Activity of M and MABC—The kinetic parameters of M and MABC for various amino acid substrates were determined (Table I). Changes in the catalytic efficiency (k_{cat}/K_m value) relative to WT are shown in Fig. 2 together with those of ATB17. The mutations of M increase the activity for all the substrates examined: a 30–40-fold increase in the catalytic efficiency was found for β-branched substrates, and a 2–6-fold increase for acidic substrates. The substrate specificity of MABC is essentially the same as that of ATB17 (Fig. 2), although small differences are observed for valine and acidic substrates: the catalytic efficiency of MABC is 2.7-fold lower and 5–6-fold higher for valine and acidic substrates, respectively, than that of ATB17 (*2*).

Effects of Each Cluster on Enzymatic Activity—The kinetic parameters of MA, MB, MC, MAB, MAC, and MABC for various amino acid substrates were also determined (data not shown). To make it easier to observe the effects of the clusters on the activity, the catalytic efficiency for each substrate was compared in all possible pairs of mutants, as shown in Fig. 3. For example, Fig. 3A shows the effects of cluster A when added to M, MB, MC, and MBC. Although there are some discrepancies, cluster A increases the catalytic efficiency especially for valine, isoleucine, and threo-

TABLE I. **Kinetic parameters of AspATs for various amino acid substrates.**

Substrate[a]	WT[b]			M			MABC		
	k_{cat} (s^{-1})	K_m (mM)	k_{cat}/K_m ($s^{-1}M^{-1}$)	k_{cat} (s^{-1})	K_m (mM)	k_{cat}/K_m ($s^{-1}M^{-1}$)	k_{cat} (s^{-1})	K_m (mM)	k_{cat}/K_m ($s^{-1}M^{-1}$)
Valine	–	–	3.4×10^{-3}[c]	–[d]	–[d]	0.098 (0.0031)	18 (0.10)	23 (1.0)	770
Isoleucine	–	–	4.9×10^{-4}[c]	–[d]	–[d]	0.018 (<0.001)	3.3 (0.10)	55 (2.0)	59
Leucine	–	–	2.4	–[d]	–[d]	47 (0.68)	52 (2.0)	5.8 (0.30)	9.0×10^{3}
Tryptophan	–	–	880	–[d]	–[d]	2.9 (0.047) $\times10^{3}$	180 (4.0)	2.7 (0.10)	6.4×10^{4}
Tyrosine	–	–	400	18 (1.0)	1.1 (0.10)	1.6×10^{4}	70 (1.0)	1.0 (0.020)	6.9×10^{4}
Phenylalanine	–	–	200	28 (3.0)	7.5 (1.1)	3.7×10^{3}	–[d]	–[d]	4.7 (<0.1)$\times10^{4}$
Histidine	–		13	–[d]	–[d]	96 (3.0)	14 (1.0)	0.64 (0.050)	2.2×10^{4}
Arginine	–		0.010	–[d]	–[d]	0.050 (0.0037)	–[d]	–[d]	77 (0.43)
Lysine	–		0.010	–[d]	–[d]	0.060 (0.0014)	–[d]	–[d]	44 (0.54)
Alanine	–	–	0.77	–[d]	–[d]	7.3 (0.15)	240 (3.0)	110 (2.0)	2.1×10^{3}
Serine	–		0.050	–[d]	–[d]	0.24 (0.0065)	1.7 (0.030)	24 (1.0)	70
Threonine	–	–	0.010	–[d]	–[d]	0.014 (<0.001)	0.88 (0.010)	17 (1.0)	52
Asparagine	–	–	1.4	1.1 (0.20)	77 (20)	15	4.6 (0.10)	0.90 (0.030)	5.1×10^{3}
Glutamine	–	–	0.74	–[d]	–[d]	14 (0.067)	140 (2.0)	25 (1.0)	5.7×10^{3}
Methionine	–	–	22	–[d]	–[d]	320 (3.9)	46 (1.0)	1.9 (0.10)	2.5×10^{4}
Aspartate	550	4.5	1.2×10^{5}	400 (93)	0.54 (0.21)	7.3×10^{5}	11 (0.20)	0.56 (0.020)	2.0×10^{4}
Glutamate	700	38	1.8×10^{4}	32 (5.0)	0.92 (0.22)	3.5×10^{4}	16 (0.20)	5.1 (0.10)	3.2×10^{3}

Standard deviations are given in parenthesis. [a]L-form amino acids were used. [b]Data from Ref. *6* except for those for β-branched amino acids. [c]Data from Ref. *13*. [d]Reactions did not show saturation kinetics in the substrate concentrations examined.

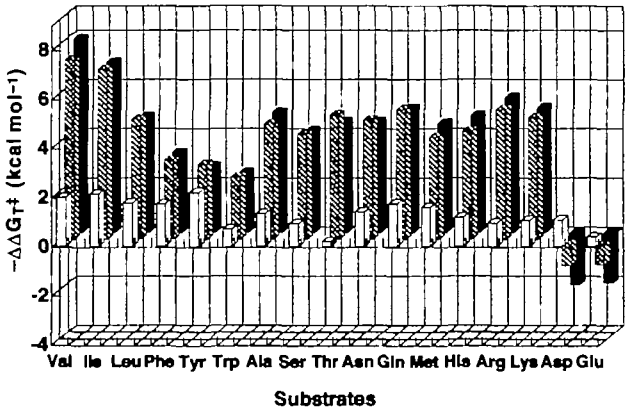

Fig. 2. **Stabilization of the activation free energy for various amino acid substrates by M (white), MABC (hatched), or ATB17 (black) relative to WT.** $-\Delta\Delta G_T^{\ddagger} = RT\ln\{(k_{cat}/K_m)_X/(k_{cat}/K_m)_{WT}\}$. Positive bars indicate that the catalytic efficiency of a mutant, X, is higher than that of WT, and negative bars indicate *vice versa*.

nine. Cluster B increases the catalytic efficiency slightly for the basic and some of the neutral amino acids, including β-branched amino acids, but decreases it significantly for acidic substrates (Fig. 3B). Cluster C increases the catalytic efficiency for all the substrates examined, not particularly for β-branched substrates, when added to almost any combination of the other mutations (Fig. 3C).

The activity of MC and MAC for aspartate could not be determined because the affinity of these mutants for oxalacetate was too high ($K_m \ll 10$ μM). Apparent rate constants (k_{app} values) for the reaction with aspartate need to be corrected for the effect of the reverse reaction (the reaction with the product, oxalacetate) (*6*). However, the high affinity for oxalacetate made it impossible to determine the parameters of these mutants for the reverse reaction and, therefore, those for the reaction with aspartate. We then measured the overall reactions with aspartate and 2-oxoleucine by coupling with the malate dehydrogenase reaction. An excess of malate dehydrogenase should remove oxalacetate from the reaction mix, eliminating the reverse reaction. The $k_{cat}^{overall}/K_m^{overall}$ value for aspartate can be compared directly with that obtained for the single-turnover reactions with aspartate (*6*). The $k_{cat}^{overall}$ values were 1.0 and 0.0078 s^{-1} for MC and MAC, respectively. These values are, however, far smaller than those estimated from the rate constants for the single-turnover reactions with aspartate and 2-oxoleucine: for example, k_{app} = 30–250 s^{-1} for 0.05–0.5 mM aspartate and k_{cat} = 500 s^{-1} for 2-oxoleucine in the case of MC. This implies that the rate-limiting step of the overall reaction is different from, and slower in rate than, that of the single-turnover reaction.

Dissociation Constants for Maleate—Cluster C decreases dramatically the K_d values for maleate (Table II): for example, the K_d values are decreased from 30 and 40 mM to 0.18 and 1.0 mM when cluster C is added to M and MA, respectively. On the other hand, cluster B increases the K_d values for maleate: the K_d value of MC is 0.18 mM, while that of MBC is 44 mM. For MABC, the spectral changes did not show saturation up to 100 mM of maleate, that is, the K_d value would be >100 mM. For MB and MAB, the absorption spectra did not change at all up to 100 mM maleate, indicating that the K_d values are > 100 mM or that these mutants do not show spectral changes upon binding maleate.

DISCUSSION

Three mutations of M, which are included in all the mutants examined in the present study, were found to increase the catalytic efficiency for all the amino acid substrates by 1–2 kcal mol^{-1} (Table I and Fig. 2). Thr11 is in the middle of an amino-terminal extension bridging the two subunits, and Val293 and Ser297 are located near the subunit interface (Fig. 1). Because the active site of AspAT is located at the subunit interface, these mutations could affect the substrate binding and/or subsequent catalytic steps by changing the arrangement of the subunits. However, the detailed mechanism remains unclear. Three mutations omitted from MABC, of which the effect on the activity was undetectable when they were individually mutated back to the wild-type

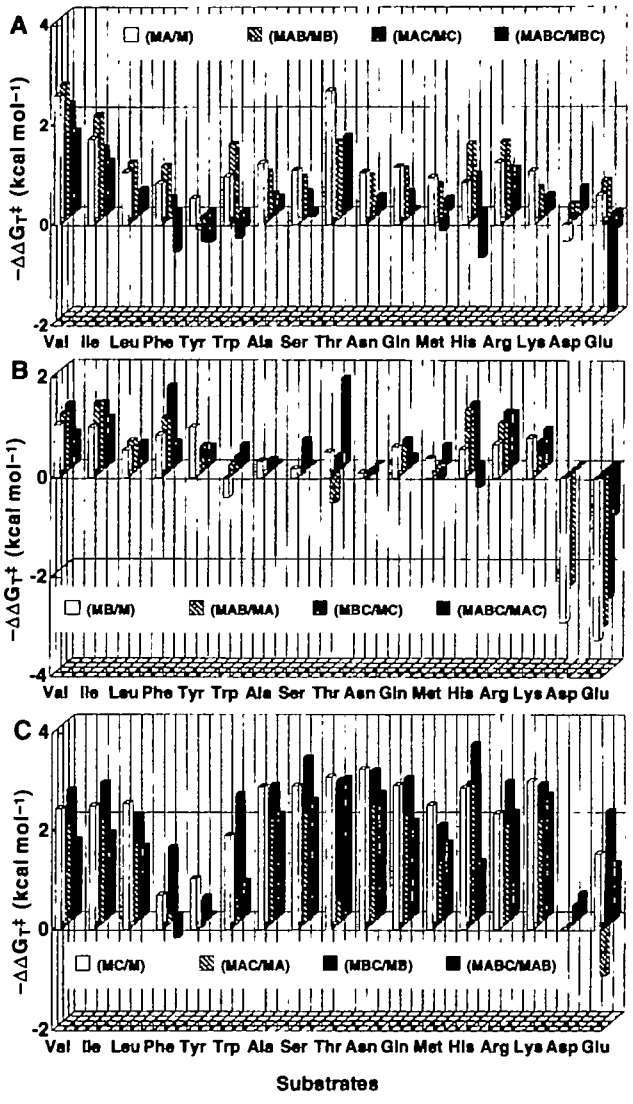

Fig. 3. **Effects of each cluster on the catalytic efficiency for various amino acid substrates.** (A) Cluster A. (B) Cluster B. (C) Cluster C. (X/Y) indicates the difference between mutants X and Y: $-\Delta\Delta G_T^{\ddagger} = RT\ln\{(k_{cat}/K_m)_X/(k_{cat}/K_m)_Y\}$. Positive bars indicate that the catalytic efficiency of X is higher than that of Y, and negative bars indicate *vice versa*. The k_{cat}/K_m values of MC and MAC for aspartate could not be determined (see text) and thus are not shown.

TABLE II. **Dissociation constants for maleate.**

AspAT	K_d (mM)
WT	10[a]
M	30 (0.99)
MA	40 (8.1)
MB	–[b]
MC	0.18 (0.051)
MAB	–[b]
MAC	1.0 (0.0034)
MBC	44 (3.7)
MABC	>100[c]

Standard deviations are given in parenthesis. [a]Taken from Ref. 6. [b]No spectral changes were observed. [c]Spectral changes did not show saturation.

sequence (*1*), show a small but significant enhancement in the catalytic efficiency for valine when mutated back simultaneously (Fig. 2), although the mechanism is totally unknown at present. In the following discussions, we speculate on how each cluster affects the structure and function of this enzyme (*10–12*) on the basis of its spatial location and the results obtained in the present and previous studies.

As shown in Fig. 3A, cluster A increases the catalytic efficiency especially for the substrates that have a bulky group, a methyl or hydroxyl group, at the β position of the side chain. Cluster A is located in a loop structure that functions as the lid of the active site. This cluster contains the Ile37Met mutation, and the crystal structure of the ATB17–valine analog complex revealed that the residue at position 37 makes direct contact with the bound substrate (*2*). Thus, the observed effects of cluster A on the activity might be explained simply by the mutation that removes the steric hindrance between the γ-methyl group of Ile37 and the bulky group at the β position of the substrate. A single revertant of ATB17, in which Met37 was mutated back to Ile, however, retained the k_{cat}/K_m value of 500 s^{-1} M^{-1} for valine (that of ATB17 is 2,100 s^{-1} M^{-1}) (*2*). This value is 80-fold larger than the corresponding value of MBC, 5.9 s^{-1} M^{-1}. Even if the effect of the three omitted mutations, a 2.7-fold increase (ATB17/MABC), is taken into consideration, the effect of cluster A is much larger than that of the Ile37Met mutation. This extra enhancement should be attributed to the other mutations of cluster A, which might affect the flexibility of the loop structure and thereby enable the upper wall of the substrate-binding site to accommodate β-branched substrates.

Cluster B increases the catalytic efficiency for β-branched substrates by about 1 kcal mol^{-1} but, more characteristically, decreases that for acidic substrates by 1–3 kcal mol^{-1} (Fig. 3B). This finding is consistent with our recent results on ATBSN (*13*), in which Gly139 and Thr142 of ATB17, corresponding to cluster B in this study, were mutated back to the wild-type residues, Ser and Asn, respectively: ATBSN recovered the activity for acidic substrates to the level of WT, while the activity for β-branched substrates was decreased by 3–5-fold. Cluster B is located at the bottom of the active site. Comparison of the crystal structures of ATB17 and ATBSN revealed that cluster B should indirectly affect the binding mode of acidic substrates through its effects on the side chain of Trp140 and on the backbone of the Pro138–Asn(Thr)142 loop (*13*). Those structural effects also result in enlargement of the substrate-binding pocket to accommodate bulky β-branched substrates. During the directed-evolution experiments, no selection pressure was applied to decrease the activity for the native, or acidic, substrates (*1, 2*). The above findings imply that the activity of ATB17 for acidic substrates was decreased by introduction of the mutations of cluster B in exchange for the increased activity for β-branched substrates.

Cluster C increases the catalytic efficiency for all the substrates, and its effects are larger than those of cluster A or B (Fig. 3C). As mentioned above, the rate-limiting steps of the single-turnover and the overall reactions with aspartate differed in MC and MAC. It is likely that the dissociation of oxalacetate from the enzyme is a rate-limiting step in these mutants: the affinity of WT for oxalacetate is very high (K_m = 35 μM) compared to the other substrates (*6*), and such strong binding would be further enhanced in

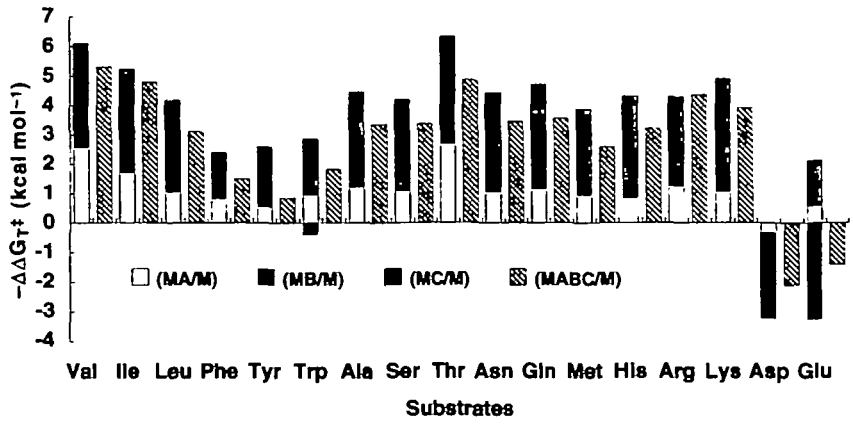

Fig. 4. **Total effects of ABC are compared to the sum of the effects of each cluster.** The contribution of M is subtracted from each $-\Delta\Delta G_T^{\ddagger}$ value of a mutant, X (X/M). Positive bars indicate that the catalytic efficiency of X is higher than that of M, and negative bars indicate *vice versa*. The k_{cat}/K_m value of MC for aspartate could not be determined (see text) and, thus, is not shown.

these mutants to the level that the rate for the dissociation of oxalacetate from the enzyme is slower than those for the chemical steps of the transformation of aspartate to oxalacetate. The K_d values for an aspartate analog, maleate, support this idea (Table II). When a substrate binds to AspAT, the small domain (residues 5–48 and 326–408, see Fig. 1) moves relative to the large domain (residues 49–325), causing gross conformational changes from an "open" form to a "closed" form (*11, 12, 14–18*). Cluster C is located around the domain interface. The findings that cluster C increases the catalytic efficiency for various amino acids regardless of the properties of their side chains and that the substrate binding is significantly enhanced in mutants containing cluster C, thus suggest that the structure of AspAT is changed to the closed form by cluster C prior to the substrate binding. Crystallographic studies confirmed that the structure of MC is the closed form in the absence of substrate analogs, while M is in the open form (H. Tada, personal communication). In the case of WT, the binding energy of the substrate should be partially consumed to elicit the structural changes. On the other hand, because the structure is pre-fixed in the closed form in mutants containing cluster C, the binding energy would be used more efficiently for catalysis, causing the increase in the catalytic efficiency by 2–3 kcal mol^{-1} (Fig. 3C). This is in good accordance with the value of the free energy required for the domain movement, 1.9 kcal mol^{-1}, estimated from another line of experiments on this enzyme (*18*). However, the question also arises of why AspAT undergoes such apparently wasteful structural changes in the first place. The present results show that if the structure is fixed to the closed form, the turnover number for the overall reaction with aspartate is decreased by more than 100-fold. Thus, AspAT might have acquired the open–closed conformational changes during its evolution to achieve smooth release of oxalacetate, while sacrificing to some extent its catalytic efficiency for the other substrates.

At the outset, we had expected to observe a strong positive cooperativity in a particular combination of the clusters. However, only weak positive cooperativity was observed in some combinations of two clusters. For example, clusters A and B enhance each other's effect on the activity for β-branched substrates (Fig. 3, A and B): the effects of cluster A or B are larger when added to MB or MA (hatched bars), respectively, than when added to M (white bars). As shown in Fig. 4, however, the effects of the three clusters introduced simultaneously were almost the same as, or even smaller than, the sum of the effects of each cluster introduced singly. The present study has revealed that (i) the three clusters have different effects on the substrate specificity, that (ii) their effects are almost independent of each other and approximately additive, that (iii) no single cluster or mutation is particularly important for the activity of ATB17, and that (iv) even the three seemingly dispensable mutations that are not included in MABC increase the activity for valine, implying that almost all of the 17 mutations might contribute to the total effect of the 10^6-fold enhancement. More detailed interpretation of the present data must await the elucidation of the crystal structures of all the mutants reported here, which is now in progress.

Amino acid residues of an enzyme would be grouped as follows: those that interact directly with the substrate or the coenzyme are defined as the first layer; those that are located immediately outside the first layer are the second layer; and the third and fourth layers are defined in the same way. Only one of the 17 mutated residues of ATB17 belongs to the first layer, and other mutated residues are in the second, third, and further outer layers. This apparently contradicts our intuition and general strategies of present-day rational protein design but might actually be very reasonable and less "dangerous" as a strategy for protein design. Most mutations in the first layer would totally "kill" the enzyme rather than modify the activity, as numerous unsuccessful attempts at protein engineering over the past decade have shown. On the other hand, mutations in the outer layers would be milder and therefore more tunable and more cumulative as demonstrated here. A few successful studies of protein design (*19–21*) and findings on catalytic antibodies (*22, 23*) support this notion. The present results are definitive evidence for the functional importance of non-active-site residues and imply that this concept should be incorporated into future protein design.

REFERENCES

1. Yano, T., Oue, S., and Kagamiyama, H. (1998) Directed evolution of an aspartate aminotransferase with new substrate specificities. *Proc. Natl. Acad. Sci. USA* **95**, 5511–5515
2. Oue, S., Okamoto, A., Yano, T., and Kagamiyama, H. (1998) Redesigning the substrate specificity of an enzyme by cumulative effects of the mutations of non-active site residues. *J. Biol. Chem.* **274**, 2344–2349

3. Kuramitsu, S., Okuno, S., Ogawa, T., Ogawa, H., and Kagamiyama, H. (1985) Aspartate aminotransferase of *Escherichia coli*: nucleotide sequence of the *aspC* gene. *J. Biochem.* **97**, 1259–1262
4. Yano, T., Kuramitsu, S., Tanase, S., Morino, Y., Hiromi, K., and Kagamiyama H. (1991) The role of His143 in the catalytic mechanism of *Escherichia coli* aspartate aminotransferase. *J. Biol. Chem.* **266**, 6079–6085
5. Inoue, Y., Kuramitsu, S., Inoue, K., Kagamiyama, H., Hiromi, K., Tanase, S., and Morino, Y. (1989) Substitution of a lysyl residue for arginine 386 of *Escherichia coli* aspartate aminotransferase. *J. Biol. Chem.* **264**, 9673–9681
6. Kuramitsu, S., Hiromi, K., Hayashi, H., Morino, Y., and Kagamiyama, H. (1990) Pre-steady-state kinetics of *Escherichia coli* aspartate aminotransferase catalyzed reactions and thermodynamic aspects of its substrate specificity. *Biochemistry* **29**, 5469–5476
7. Karmen, A. (1955) A note on the spectrophotometric assay of glutamic oxalacetate transaminase in human blood serum. *J. Clin. Invest.* **34**, 131–133
8. Faesella, P., Giartosio, A., and Hammes, G.G. (1966) The interaction of aspartate aminotransferase with α-methylaspartic acid. *Biochemistry* **5**, 197–202
9. Fonda, M.L. and Johnson, R.J. (1970) Computer analysis of spectra of enzyme-substrate and enzyme-inhibitor complexes involving aspartate aminotransferse. *J. Biol. Chem.* **245**, 2709–2716
10. Kirsch, J.F., Eichele, G., Ford, G.C., Vincent, M.G., Jansonius, J.N., Gehring, H., and Christen, P. (1984) Mechanism of action of aspartate aminotransferase proposed on the basis of its spatial structure. *J. Mol. Biol.* **174**, 497–525
11. McPhalen, C.A., Vincent, M.G., and Jansonius, J.N. (1992) X-ray structure refinement and comparison of three forms of mitochondrial aspartate aminotransferase. *J. Mol. Biol.* **225**, 495–517
12. Okamoto, A., Higuchi, T., Hirotsu, K., Kuramitsu, S., and Kagamiyama, H. (1994) X-ray crystallographic study of pyridoxal 5′-phosphate-type aspartate aminotransferases from *Escherichia coli* in open and closed form. *J. Biochem.* **116**, 95–107
13. Oue, S., Okamoto, A., Yano, T., and Kagamiyama, H. (2000) Co-crystallization of a mutant aspartate aminotransferase with a C5-dicarboxylic substrate analog: structural comparison with the enzyme–C4-dicarboxylic analog complex. *J. Biochem.* **127**, 337–343
14. Borisov, V.V., Barisova, S.N., Kachalova, G.S., Sosfenove, N.I. and Vainshtein, B.K. (1985) X-ray studies of chicken cytosolic aspartate aminotransferase in Transaminase (Christen, P. and Metzler, D.E., eds.) pp. 155–164 Wiley and Sons, New York
15. Arnone, A., Rogers, P.H., Hyde, C.C., Briley, P.D., Metzler, C.M., and Metzler, D.E. (1985) Pig cytosolic aspartate aminotransferase: the structures of the internal aldimine, external aldimine, and ketimine and of the β subform in *Transaminases* (Christen, P. and Metzler, D.E., eds.) pp. 138–155, Wiley and Sons, New York
16. Kamitori, S., Okamoto, A., Hirotsu, K., Higuchi, T., Kuramitsu, S., Kagamiyama, H., Matsuura, Y., and Katsube, Y. (1990) Three-dimensional structures of aspartate aminotransferase from *Escherichia coli* and its mutant enzyme at 2.5 Å resolution. *J. Biochem.* **108**, 175–184
17. Kawaguchi, S., and Kuramitsu, S. (1998) Thermodynamics and molecular simulation analysis of hydrophobic substrate recognition by aminotransferases. *J. Biol. Chem.* **273**, 18353–18364
18. Ishijima, J., Nakai, T., Kawaguchi, S., Hirotsu, K., and Kuramitsu, S. (2000) Free energy requirement for domain movement of an enzyme. *J. Biol. Chem.* **275**, 18939–18945
19. Hedstrom, L., Szilagyi, L., and Rutter, W.J. (1992) Converting trypsin to chymotrypsin: the role of surface loops. *Science* **255**, 1249–1253
20. Onuffer, J.J. and Kirsch, J.F. (1995) Redesign of the substrate specificity of *Escherichia coli* aspartate aminotransferase to that of *Escherichia coli* tyrosine aminotransferase by homology modeling and site-directed mutagenesis. *Protein Sci.* **4**, 1750–1757
21. Malashkevich, V.N., Onuffer, J.J., Kirsch, J.F., and Jansonius, J.N. (1995) Alternating arginine-modulated substrate specificity in an engineered tyrosine aminotransferase. *Nat. Struct. Biol.* **2**, 548–553
22. Patten, P.A., Gray, N.S., Yang, P.L., Marks, C.B., Wedemayer, G.J., Boniface, J.J., Stevens, R.C., and Schultz, P.G. (1996) The immunological evolution of catalysis. *Science* **271**, 1086–1091
23. Wedemayer, G.J., Patten, P.A., Wang, L.H., Schultz, P.G., and Stevens, R.C. (1997) Structural insights into the evolution of an antibody combining site. *Science* **276**, 1665–1669